Oecologia (2022) 198:933–946
https://doi.org/10.1007/s00442-022-05156-1

PHYSIOLOGICAL ECOLOGY – ORIGINAL RESEARCH

Tree growth sensitivity to climate varies across a seasonal precipitation gradient

Larissa Yocom[1] · Kiona Ogle[2,3] · Drew Peltier[3] · Paul Szejner[4,5] · Yao Liu[6,7] · Russell K. Monson[5,8]

Received: 19 July 2021 / Accepted: 28 March 2022 / Published online: 17 April 2022

Abstract

Spatial patterns of precipitation in the southwestern United States result in a complex gradient from winter-to-summer moisture dominance that influences tree growth. In response, tree growth exhibits seasonal-to-annual variability that is evident in the growth of whole tree rings, and in sub-annual sections such as earlywood and latewood. We evaluated the influence of precipitation and temperature on the growth of *Pinus ponderosa* trees in 11 sites in the southwestern US. Precipitation during the year of growth and the prior year accounted for about half of the climate influence on annual growth, with the other half reflecting conditions 2–4 years prior to growth, indicating that individual trees do indeed exhibit multi-year "memory" of climate. Trees in wetter sites exhibited weaker influence of past precipitation inputs, but longer memory of climatic variability. Conversely, trees in dry sites exhibited shorter memory of long-term climatic variability, but greater sensitivity to past precipitation effects. These results are consistent with the existence of complex interactions between endogenous (phenotype) effects and exogenous (climate) effects in controlling climate memory in trees. After accounting for climate, residual variability in latewood growth was negatively correlated with earlywood growth, indicating a potential tradeoff between latewood versus earlywood growth. This study provides new insights that will assist the accurate prediction of woody biomass growth and forest carbon sequestration across a southwestern US precipitation gradient.

Keywords Bayesian · Dendrochronology · Memory · Monsoon · *Pinus ponderosa*

Communicated by Christiane Roscher.

✉ Larissa Yocom
larissa.yocom@usu.edu

1 Department of Wildland Resources and the Ecology Center, Utah State University, 5230 Old Main, Logan, UT, USA

2 School of Informatics, Computing, and Cyber Systems, Northern Arizona University, Flagstaff, AZ, USA

3 Department of Biological Sciences, Northern Arizona University, Flagstaff, AZ, USA

4 Instituto de Geología, Universidad Nacional Autónoma de México, México City, México

5 Laboratory of Tree-Ring Research, University of Arizona, Tucson, AZ, USA

6 Environmental Sciences Division and Climate Change Science Institute, Oak Ridge National Laboratory, Oak Ridge, TN, USA

7 Present Address: Department of Geography and Environmental Sciences, Northumbria University, Newcastle upon Tyne, UK

8 Department of Ecology and Evolutionary Biology, University of Arizona, Tucson, AZ, USA

Introduction

Annual tree-ring growth integrates the interactions of numerous physiological processes with climate variability at sub-annual to multi-year time scales (Fritts 1976; Salzer and Kipfmueller 2005; Stahle et al. 2009; Griffin et al. 2013; Peltier et al. 2016, 2018). The responsiveness of tree-ring widths to climate during the year of ring formation, and often during the prior year, has enabled their use in reconstructing past patterns of climate variables, such as precipitation and temperature (e.g., Salzer et al. 2005; Stahle et al. 2009; Griffin et al. 2011, 2013; Esper et al. 2018). However, annual ring widths are also influenced by climate over multiple years, whereby climate signals from several seasons prior to ring formation are detectable (Ogle et al. 2015; Peltier et al. 2016, 2018; Marqués et al. 2021).

Within individual annual rings in trees from temperate ecosystems, particularly conifers, there is variation in wood cell structure that reflects seasonal climate variations. Light-colored earlywood consists of large, thin-walled cells formed early in the growing season. Darker-colored latewood is

formed later in the growing season and is characterized by smaller lumen area with thicker cell walls. Sub-annual patterns of earlywood and latewood can be used to inform intra-annual climate-growth relationships, particularly in regions with strong seasonal climatic patterns (Griffin et al. 2013; Babst et al. 2016; Monson et al. 2018; Szejner et al. 2016). Earlywood growth can be related to temperature (e.g., Zhang et al. 2021) but is often correlated with the amount of winter and spring precipitation received (for example, November through May; [Stahle et al. 2009]). Latewood width has been found to record a summer precipitation signal, especially if its dependence on earlywood growth is statistically removed (Stahle et al. 2009; Griffin et al. 2013; Szejner et al. 2018). It has been thought that earlywood and latewood are dependent on different sources of water because ring widths and seasonally recorded oxygen isotopes in the two types of wood have been found to correlate with precipitation in different seasons: winter precipitation for earlywood, and summer rainfall for latewood (Belmecheri et al. 2018; Ziaco et al. 2018; Szejner et al. 2018). However, there has been little research on the extent to which the growth of earlywood and latewood in the current year integrates climate over multiple prior years, or potential carbon allocation trade-offs between tree investment in earlywood versus latewood growth once climate-specific effects have been reconciled.

Summer rains in the southwestern United States (hereafter, "Southwest") are delivered by the North American Monsoon (NAM) climate system (Fig. 1). The NAM is characterized by frequent convective rain events that generally begin in early July in the Southwest and continue through September, following very dry conditions in May and June (Adams and Comrie 1997; Higgins et al. 1997). There is high variability in NAM precipitation at seasonal, annual, and decadal time-scales (Higgins et al. 2003; Adams et al. 2014), and in the annual timing of NAM onset (Higgins et al. 1999). Geographically, there is a northwest-to-southeast gradient from winter-to-summer moisture dominance in the Southwest, with summer rainfall dominant in the southeast and winter precipitation dominant in the northwest (Fig. 1a). At the extreme of the gradient, >70% of annual rainfall is contributed by the NAM in parts of southern Arizona and New Mexico (Douglas et al. 1993; Szejner et al. 2016). Thus, depending on location, the NAM provides a significant moisture resource that potentially influences the growth, structure, and community composition of vegetation in the Southwest (Neilson 1987).

However, there are other patterns in precipitation across the region as well. There is a gradient in total annual precipitation from east-to-west, with greater precipitation in eastern New Mexico, grading to less precipitation in western Arizona. Within these regional patterns, precipitation increases with elevation (Fig. 1b). Variability of annual precipitation amount is highly correlated with total annual precipitation amount—i.e., there is generally a higher standard deviation in precipitation among years in areas with higher mean annual precipitation (Fig. 1c). Because of the strong gradients in summer and annual precipitation across the region and the variability in precipitation inherent in the regional climate system, the Southwest represents an excellent location to test the influence of seasonal precipitation as well as its variability on tree growth, including in the sub-annual components of tree rings.

The stochastic antecedent modeling (SAM) framework was developed to evaluate antecedent factors (e.g., climate drivers) and their influence on physiological processes such as tree growth (Ogle et al. 2015; Peltier et al. 2018). The SAM framework provides a quantitative method of analyzing the importance of "ecological memory"—that is, the influence of antecedent conditions on current processes (Ogle et al. 2015). An advantage of the SAM approach is that the strength and temporal lags of each variable driving growth can be evaluated simultaneously. Thus, we can

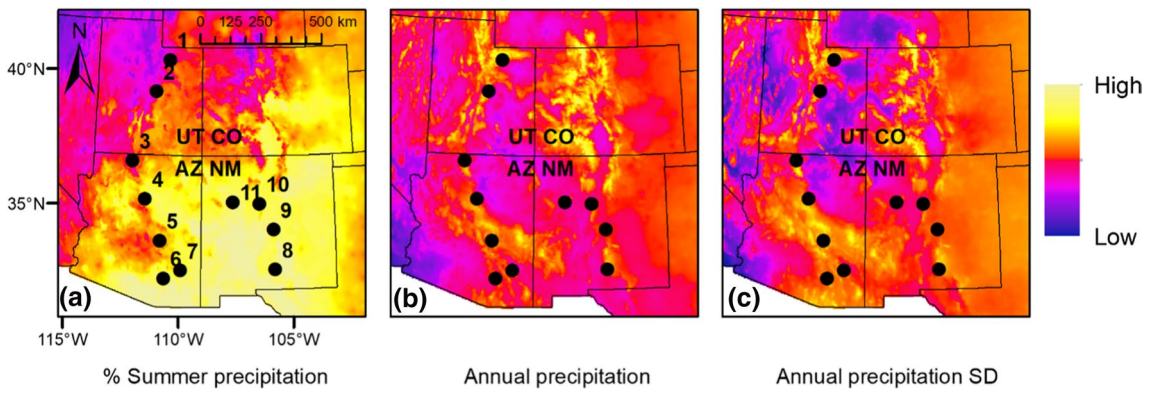

Fig. 1 Eleven sites where *Pinus ponderosa* trees were sampled in the southwestern USA (UT: Utah, AZ: Arizona, NM: New Mexico, CO: Colorado). Color gradient represents **a** % precipitation that falls in summer (July, August, and September), **b** mean total annual precipitation, and **c** standard deviation of precipitation. See Table S1 for details on each site

reconstruct the roles of multiple exogenous and endogenous processes in the ecophysiological memory of trees. In the current study, we applied this approach to annual and intra-annual tree growth increments using *Pinus ponderosa* trees distributed across a broad geographic precipitation gradient selected specifically to study variation in tree growth processes across varied precipitation conditions. In doing so, we addressed three primary questions: (1) Over what time scales (e.g., past monthly, seasonal, or annual periods) are climate influences on tree growth evident? (2) Do tree growth sensitivity to climate and ecological memory vary across the precipitation gradient? (3) Do earlywood and latewood growth differ in their sensitivities to climate and climatic memory? Addressing these questions will provide insight into the complexities of the responses of earlywood, latewood, and whole rings to antecedent climate, helping us to disentangle the endogenous and exogenous mechanisms underlying tree growth responses to variation in climate. Our study has implications for understanding drought impacts and forest functioning, in general, given current and future climatic variation, and within the more specific context of regional climate attributes.

Methods

Data description

To answer our questions, we used a set of tree cores previously collected for a related tree-ring isotope study (Szejner et al. 2016). Tree cores with at least 5 decades of growth were collected from ponderosa pine trees (*Pinus ponderosa* Dougl. ex Laws.) in 11 sites, with five sites in AZ, four in NM, and two in UT (Fig. 1; Szejner et al. 2016). Sites were located in ponderosa pine-dominated landscapes with low tree-to-tree canopy competition. Healthy, medium-sized trees were selected at each site (Szejner et al. 2016). Using a 5 mm increment borer, 2–3 cores were taken from each of 128 selected trees for a total of 266 cores (Table S1). In the laboratory, cores were crossdated using standard dendrochronology techniques (Stokes and Smiley 1968), and total ring, earlywood, and latewood widths of each ring were measured (Szejner et al. 2016).

Monthly precipitation and mean maximum monthly temperature data from 1895 to 2014 for each site were extracted from the PRISM gridded climate dataset (PRISM 2018) at the 30-m pixel resolution representing each site location. We considered using other climate indices (e.g., Palmer Drought Severity Index, vapor pressure deficit, minimum monthly temperature), but exploratory analyses of relationships between ring widths and these alternative indices led us to focus on simple precipitation and temperature variables. Precipitation and temperature, while not wholly representative of drought stress, are consistently and reliably measured and widely interpreted, and they include no built-in time-lags (such as those within PDSI).

Statistical model description

We used the stochastic antecedent modeling (SAM) approach developed by Ogle et al. (2015), which has been used in multiple applications (e.g., Liu et al. 2019; Guo et al. 2020), including several applications to estimate the effects that climatic variables have on tree growth as well as the time scales over which such variables influence growth (Peltier et al. 2018, 2022; Peltier and Ogle 2019; Marqués et al. 2021). This model regresses ring widths (growth) on antecedent climate variables, while simultaneously estimating the time-scales over which the antecedent variables are defined, thus providing insight into lags and memory effects. That is, climatic variables affecting growth, as well as previous ring-width values, are used to construct antecedent variables, which themselves are defined as weighted averages of past observed values. The antecedent variables serve as covariates in the regression model, where each antecedent variable has its own effect parameter.

We assumed that observed, log-transformed ring widths, $r = \log(\text{ring width} + 1)$, for each core, c, and year, y, were normally distributed around the mean, $\mu_{y,c}$, with variance, σ^2:

$$r_{y,c} \sim \text{Normal}(\mu_{y,c}, \sigma^2) \tag{1}$$

Note that 1 was added to each ring width before log transforming to account for zero values due to missing rings (0.4% of rings were missing). We modeled μ as a function of ring age (A), antecedent precipitation (P^{ant}; see Eq. 5), antecedent maximum temperature (T^{ant}; see Eq. 5), the $P^{\text{ant}} \times T^{\text{ant}}$ two-way interaction, and log-scale prior ring width (rw^{ant}):

$$\mu_{y,c} = \varepsilon_c + \alpha_{t(c),2} A_{y,c} + \alpha_{t(c),3} P^{\text{ant}}_{y,s(c)} + \alpha_{t(c),4} T^{\text{ant}}_{y,s(c)} + \alpha_{t(c),5} P^{\text{ant}}_{y,s(c)} \times T^{\text{ant}}_{y,s(c)} + \alpha_{t(c),6} rw^{\text{ant}}_{y,c}. \tag{2}$$

The nested notation $t(c)$ and $s(c)$ denote the tree, t, and site, s, corresponding to core c, respectively. Again, the model for μ in Eq. (2) is essentially a linear regression, conditional on the antecedent covariates and ring age (hence, detrending for age is accomplished simultaneously within the model). Because μ represents log-transformed ring widths, the "linear age" effect on the log scale actually represents an exponential age function. The model includes a core-level intercept, or random effect (ε_c), that is modeled hierarchically around a tree-level intercept term, $\alpha_{t,1}$:

Table 1 Summary of coefficients in the stochastic antecedent modeling (SAM) regression model (Eq. 2)

Symbol		Definition
Tree-level	Site-level	
$\alpha_{t,1}$	$a_{s,1}$	Intercept; predicted growth at average age and climate
$\alpha_{t,2}$	$a_{s,2}$	Age effect
$\alpha_{t,3}$	$a_{s,3}$	Antecedent precipitation effect
$\alpha_{t,4}$	$a_{s,4}$	Antecedent temperature effect
$\alpha_{t,5}$	$a_{s,5}$	Antecedent precipitation × antecedent temperature effect
$\alpha_{t,6}$	$a_{s,6}$	Prior ring width effect
$\alpha_{t,7}$	$a_{s,7}$	Effect of earlywood on latewood growth (only in latewood model)

The subscripts t and s denote tree t and site s

$$\varepsilon_c \sim \text{Normal}(\alpha_{t(c),1}, \sigma_\varepsilon^2). \tag{3}$$

See Table 1 for a summary of the parameters (coefficients) in Eqs. (2) and (3).

To account for the field sampling scheme, where trees were sampled in 11 sites, we specified hierarchical priors for the tree-level α parameters, which varied around site-level means (a); site-level means were modeled as varying around a population- or species-level mean (a^*). Thus, for parameter $k = 1, 2, \ldots, 6$, tree t, and site s:

$$\begin{aligned} \alpha_{t,k} &\sim \text{Normal}(a_{s(t),k}, \sigma_{\alpha_k}^2), \\ a_{s,k} &\sim \text{Normal}(a_k^*, \sigma_{a_k}^2). \end{aligned} \tag{4}$$

where $s(t)$ denotes site s associated with tree t. The variance terms ${\sigma_\alpha}^2$ and ${\sigma_a}^2$ describe how parameter k varies among trees within each site and among sites, respectively. Finally, we assigned relatively non-informative priors to the population-level means and all standard deviation terms (σ in Eq. (1), σ_ε in Eq. (3), and σ_α and σ_a in Eq. (4)). That is, each ${a_k}^*$ was assigned a wide, normally distributed prior with mean 0 and standard deviation 10,000; each standard deviation term was assigned a wide, uniform prior between 0 and 100.

Defining the model covariates

The age of each tree t at the time of coring (i.e., the "final age") was not always known given that many cores did not include the pith. Thus, we treated the final age, A^{final}, of each tree as unknown, resulting in unknown age for each ring (A) such that:

$$A_{y,c} = A_{t(c)}^{\text{final}} - \delta_y, \tag{5}$$

where δ_y is the number of rings produced after year y; e.g., if the most recent ring is 2012, then $\delta_y = 0, 1, 2, \ldots$, when y corresponds to 2012, 2011, 2010, …, respectively. Again, A^{final} is treated as an unknown quantity that is estimated for each tree (δ is known data). Thus, we assigned a vague (wide) uniform prior to each A_t^{final} with the lower limit set equal to the number of rings measured in tree t and the upper limit set to 1000.

We centered covariates to improve parameter interpretation and model convergence. Ring age, A, was centered about the estimated average ring age, $\overline{A}$ (~120 years), in all cores across all 11 sites; the antecedent climate variables were centered about the mean monthly values for each site ($\overline{P}$ and $\overline{T}$); and the antecedent ring widths, rw^{ant}, were centered about the average ring width recorded for each tree ($\overline{rw}$). Thus, the intercept (e.g., $\alpha_{t,1}$ in Eq. (3)) is the predicted, log-scale growth of tree t at an age of 120 years under average climatic and growth conditions (Table 1).

Furthermore, the antecedent variables (P^{ant}, T^{ant}, and rw^{ant}) are defined as weighted averages of past monthly (P^{ant} and T^{ant}) and yearly (rw^{ant}) values. For $X = P$ or T, the antecedent climate variables are defined as:

$$X_{y,s}^{\text{ant}} = \sum_{j=0}^{4} \sum_{m=1}^{12} \omega_{j,m,s,X} X_{y-j,m,s}. \tag{6}$$

The antecedent importance weights, ω, are unknown and determined by fitting the model to the tree-ring and climate data. The importance weights can reveal time scales in the influences of past climate. Each climate variable at each site gets its own set of importance weights, as indicated by the s (site) and X subscripts on ω. The term $X_{y\text{-}j,m,s}$ is the precipitation total or maximum temperature for month m ($m = 1, 2, \ldots, 12$ for Jan., Feb., …, Dec.), j years prior to the current year y, in site s. The weighted monthly climate values are summed over all months ($m = 1, 2, \ldots, 12$), from $j = 0$ (year of ring formation) to $j = 4$ (4 years prior). The weights for current-year October through December ($m = 10, 11, 12$; $j = 0$) were set to 0 since we assumed the climate in these months occurred after growth ended and had no effect on current-year ring widths (McDowell et al. 2010). Monthly importance weights were estimated individually for the year of ring formation and 1 year prior ($j = 0$ and 1), but estimated in blocks of 2 months for two years prior to growth ($j = 2$)

and in blocks of 3 months for 3 and 4 years prior to growth ($j = 3$ and 4; see fig.2 in Peltier et al. 2018). This results in a total of 35 importance weights, which were constrained to sum to 1 for each climate variable within each site; hence, each $\omega_{j,m,s,X}$ indicates the relative importance of climate variable X at site s in a particular time period (j and m).

Antecedent ring width, rw^{ant} in Eq. (2), was calculated similarly to the antecedent climate variables, but since ring widths are only reported at an annual scale, rw^{ant} is given by:

$$rw_{y,c}^{\text{ant}} = \sum_{j=1}^{4} w_{j,s} rw_{y-j,c}. \quad (7)$$

The $rw_{y\text{-}j,c}$ term denotes the annual ring width (not log transformed) grown j years ($j = 1, 2, 3, 4$) prior to the current year's growth in year y. Here, $w_{j,s}$ denotes the relative importance of growth (ring width) j years prior to the current year at site s. Again, these antecedent weights were constrained to sum to 1 for each site s.

We assigned each group of antecedent importance weights—for precipitation, temperature, and past ring widths—a vague Dirichlet prior, *Dirichlet*(1,1,…,1), resulting in the prior expectation that all weights were the same (Ogle et al. 2015; Peltier et al. 2018). This prior also ensures that the weights sum to 1 and are each between 0 and 1.

Model implementation and further analyses

We implemented the above model, Eqs. (1)–(7), separately for whole-ring, earlywood, and latewood ring widths. The model structure was the same for the whole-ring and earlywood analyses, but it was modified for the latewood model by incorporating the earlywood ring width of the same year as a predictor in Eq. (2), with its corresponding effect parameter, $\alpha_{t(c),7}$ (e.g., Griffin et al. 2011), which was also assigned a hierarchical prior following Eq. (4). This was done so that we could estimate the conditional effect of earlywood growth given that climate, ring age, and past ring width effects are simultaneously accounted for. We centered earlywood ring widths about the average value reported for each tree t.

For the climate variables, we performed several calculations with the importance weights to provide greater insight into time-scales of influence and memory. For example, we computed annual importance weights by summing monthly importance weights, $\omega_{j,m,s,X}$ in Eq. (6), over all months m within each year j. For each climate variable, we also determined the number of months it took for each site to reach 50% of its cumulative monthly importance weight, which we refer to as M_{50}, following the definition in Ogle et al. (2015). M_{50} provides an index of the length of the climate memory (Ogle et al. 2015). Since months 10–12 (Oct–Dec) of the current year are assigned importance weight values of zero, this restricts M_{50} to be greater than 3 months. These quantities are computed within the model code (see below), enabling posterior estimates of each.

Using a high-performance computing cluster, we ran the model via the Bayesian software JAGS 4.2.0 (Plummer 2003) in R (R Core Team 2021) with the packages 'rjags' (Plummer 2013) and 'coda' (Plummer et al. 2006). Following standard practice to use multiple chains, we assigned different initial values to three parallel Markov chain Monte Carlo (MCMC) sequences and ran the sequences until they converged (>100,000 iterations). After convergence, we used a posterior sample size of ≥3000 relatively independent posterior samples after thinning to obtain parameter estimates, including the posterior mean, standard deviation, and 95% credible interval (CI), defined by the 2.5th and 97.5th percentiles of the posterior samples.

Post-analysis growth responses across climatic gradients

We used the posterior parameter estimates to explore relationships between parameters describing the sensitivity of growth to climate (i.e., the site-level $a_{s,3}$, $a_{s,4}$, and $a_{s,5}$ effects; Table 1) and factors related to the variability in precipitation across the Southwest such as average precipitation, % of precipitation that falls in the summer, and annual, summer, and winter precipitation variability. For seasonal climate variables, we defined winter as December through March, and summer as July through September (Higgins et al. 1997). We performed a simple model comparison among these post-hoc models with single variables, which were linear regressions of the site-specific posterior parameter means versus site-level covariates.

Results

Model fit

A regression of observed versus mean predicted values of $r = \log(\text{ring width} + 1)$ resulted in coefficients of determination (R^2) of 0.86, 0.84, and 0.74 for the whole ring, earlywood, and latewood models, respectively (Fig. S1). A regression of observed versus predicted values of raw ring widths resulted in R^2 values of 0.84, 0.82, and 0.70, respectively (Fig. S1). Site-level R^2 ranged from 0.40 to 0.92 (Table S2), with the best model fits occurring for sites in the northern portion of the study area (sites 1, 2, 3, and 4, but also site 9; Table S2 and Fig. 1).

Parameter estimates

Based on the population of sites studied here, overall, tree growth was positively associated with precipitation (Fig.

S2c), the precipitation × temperature interaction (Fig. S2e), and prior growth (Fig. S2f). Conversely, overall tree growth was negatively associated with age (Fig. S2b) and earlywood growth (for the latewood model; Fig. S2g). Given the large variation in site-specific responses to temperature (Fig. 2d), the overall temperature effect tended towards negative, but was non-significant (Fig. S2d).

Focusing on the site-specific parameter estimates (e.g., Fig. 2), baseline annual growth ($a_{s,1}$, back-transformed to mm) under average climate conditions varied by a factor of 2.4, ranging from 1.68 mm ± 0.08 (posterior mean ± SD; site 4, northern Arizona [AZ]) to 4.00 mm ± 0.22 (site 7, southern AZ) for the whole ring (Fig. 2a). Baseline earlywood growth was slightly less than whole-ring growth, and varied by a factor of 1.9 (range 1.53 mm ± 0.08 [site 4] to 2.91 mm ± 0.14 [site 8, southern New Mexico (NM)]), but baseline latewood growth was more consistent across sites with a mean of 0.37 mm (range 0.32 ± 0.03 [site 1, northern Utah (UT)] to 0.47 ± 0.03 [site 8]) (Fig. 2a). As expected, ring widths decreased with age for whole rings and earlywood ($a_{s,2} < 0$ in 9 sites in each model), but a smaller age effect was obvious in latewood widths ($a_{s,2} < 0$ for 5 sites and no significant relationship, $a_{s,2} \cong 0$, for 6 sites; Fig. 2b). Prior growth had a significant positive effect ($a_{s,6} > 0$) on ring width in all sites for all ring types (Fig. 2f). While earlywood and latewood widths were positively correlated with each other on initial study (Fig. S3), once the effects of climate, ring age, and prior ring width were accounted for, latewood width was significantly and negatively related to earlywood width ($a_{s,7} < 0$) of the same year in every site

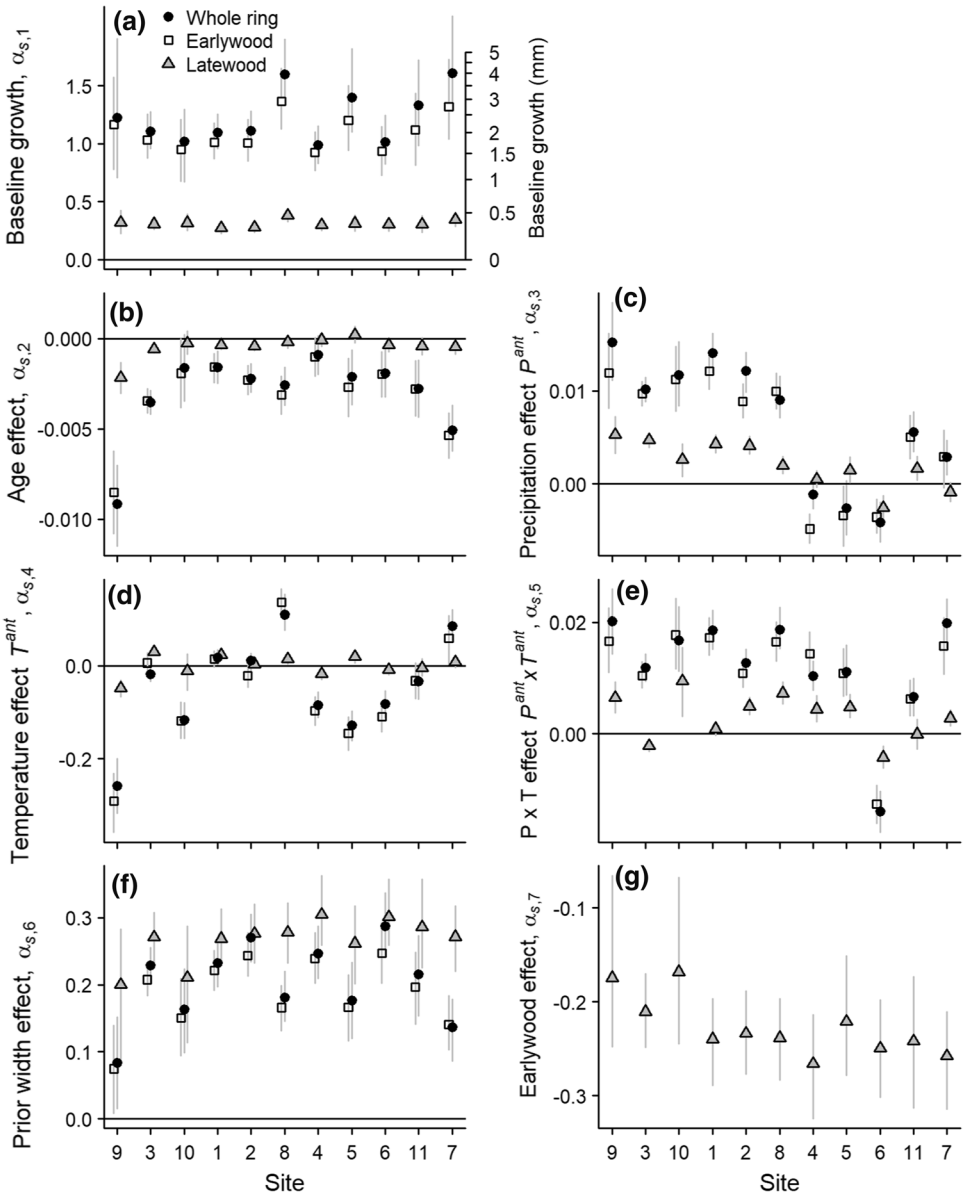

Fig. 2 Posterior means (*symbols*) and 95% Bayesian credible intervals (*whiskers*) for study-level parameters, including **a** baseline growth (intercept; $a_{s,1}$) and the effects of **b** age (A; $a_{s,2}$), **c** antecedent precipitation (P^{ant}; $a_{s,3}$), **d** antecedent temperature (T^{ant}; $a_{s,4}$), **e** the $P^{ant} \times T^{ant}$ interaction ($a_{s,5}$), **f** prior ring-width ($a_{s,6}$), and **g** earlywood width for latewood ($a_{s,7}$); see Eq. (2) and Table 1. Parameters with CIs not crossing zero are interpreted as reflecting important ("significant") effects. Sites are ordered by mean annual precipitation (low to high)

(Fig. 2g). Although sites were modeled hierarchically, which allows for sites with small sample sizes to be informed by other sites, those sites with fewer trees sampled were typically associated with more uncertain parameter estimates (wider CIs). This illustrates that the model is accounting for the unbalanced sample design.

Antecedent precipitation (P^{ant}) had a significant positive effect ($a_{t,3} > 0$) on whole-ring growth at eight sites and a significant negative effect ($a_{t,3} < 0$) in site 6, the most southern site (Fig. 2c). Conversely, the direction of the antecedent temperature (T^{ant}) effects varied, with a significant positive effect ($a_{t,4} > 0$) occurring in three sites and a significant negative effect ($a_{t,4} < 0$) in six sites (Fig. 2d). While some sites were associated with non-significant P^{ant} (sites 4 and 5) or T^{ant} (sites 2 and 11) main effects, the $P^{ant} \times T^{ant}$ interaction effect ($a_{t,5}$) was significant across all sites (Fig. 2e), indicating that P^{ant} and T^{ant} are significant predictors of growth, either via their direct (main) effects and/or via their interaction with each other. In particular, the $P^{ant} \times T^{ant}$ interaction effect for whole rings was significantly different from zero for all sites; in all sites except one, the effect was positive, and in site 6 (southern AZ), it was negative. The generally positive $P^{ant} \times T^{ant}$ effect indicates that warmer conditions (higher T^{ant}) increase the (positive) sensitivity of growth to P^{ant}, or, alternatively, drier conditions (lower P^{ant}) enhance the negative effect of T^{ant} on growth. Effects of P^{ant}, T^{ant}, and $P^{ant} \times T^{ant}$ on earlywood growth were similar to the whole-ring effects in sign, magnitude, and significance, but they were generally of lower magnitude for latewood growth (Fig. 2c–e).

Antecedent importance weights

For most sites, the year of ring formation and the prior year had the highest annual precipitation weights for all three models (whole ring, earlywood, and latewood), indicating that growth is primarily governed by fairly recent precipitation inputs (Fig. S4). However, there were some exceptions; precipitation 2 years prior to growth was most important for whole-ring widths in sites 6 and 7 (southern AZ) (Fig. S4a) and for earlywood at those two sites as well as site 4 (northern AZ) (Fig. S4b). In site 5 (central AZ), precipitation received in all 5 years had nearly equal influence (weights) on whole ring and earlywood growth. Precipitation received in the year prior to growth was more important than the year of growth for predicting latewood width in 10 sites; only in site 2 (central Utah [UT]) was the annual weight highest in the year of growth (Fig. S4c). Temperature weights were also generally highest for the year of growth in all three models, with some exceptions (Fig. S4d–f). It is worth noting that if we had defined the annual period as October through September, annual weights would have been even higher for the current year.

Consistent with the annual importance weights, individual monthly weights were also generally highest in the year of and the year prior to ring formation, but variation in the monthly weights points to specific periods that are most important for predicting growth (Figs. S5a, S5b, S5c). In sites 1, 2, 3, and 4 (UT and northern AZ), which are among the coolest sites with the lowest annual precipitation, winter precipitation in the year of growth was important for whole ring (Fig. S5a) and earlywood growth (Fig. S5b), while in sites 5 and 6 (southern AZ), which are among the warmest sites, with most annual precipitation, winter precipitation two years prior to growth was more important than winter precipitation in the year of growth. For whole-ring and earlywood widths, temperature in the spring months during the year of ring formation was influential in most sites (Fig. S5a, S5b). For latewood widths (Fig. S5c), precipitation in the winter prior to ring formation was often as or more important than summer precipitation during the current growing season. Temperature during the spring and summer of the current growing season was influential in most sites.

At the sites with the highest precipitation and variability in precipitation (sites 5, 6, and 7 in southern AZ; Table S1), whole-ring widths had the longest climatic memory as measured by the M_{50} index for P^{ant} (Fig. 3a, Fig. S6a). Climatic memory of earlywood growth was similar to that of the whole-ring, although site 4 (northern AZ), which is characterized by moderate precipitation variability, had the longest earlywood M_{50} (31 months) for P^{ant} (Fig. 3d, Fig. S6b). There was less variation among sites in the latewood M_{50} values, which were generally unrelated to site-level precipitation variability (Fig. 3d, Fig. S6c).

Sites with short climatic memory tended to have a positive, strong sensitivity to precipitation, but a negative sensitivity to temperature (Fig. S7). With increasing M_{50} for P^{ant}, the precipitation effects (P^{ant}; $a_{s,3}$) took on smaller, less positive values or even negative values. However, with increasing M_{50} for T^{ant}, the T^{ant} effects ($a_{s,4}$) took on less negative values or even positive values. In summary, the magnitudes of the P^{ant} and T^{ant} main effects, which are indices of the climate sensitivities of growth, tended to be larger (more sensitive) for sites characterized by shorter memory (lower M_{50}) (Fig. S7).

Evaluation of site-level responses across climatic gradient

Site-level sensitivity of growth to antecedent precipitation (i.e., as quantified by $a_{s,3}$; Table 1) varied in relation to site-level climate characteristics (Fig. 4). Notably, the sensitivity of whole-ring growth to antecedent precipitation at average temperature conditions, as described by the site-level P^{ant} main effect ($a_{s,3}$), was not related to the proportion of precipitation falling in the summer months (Table S3).

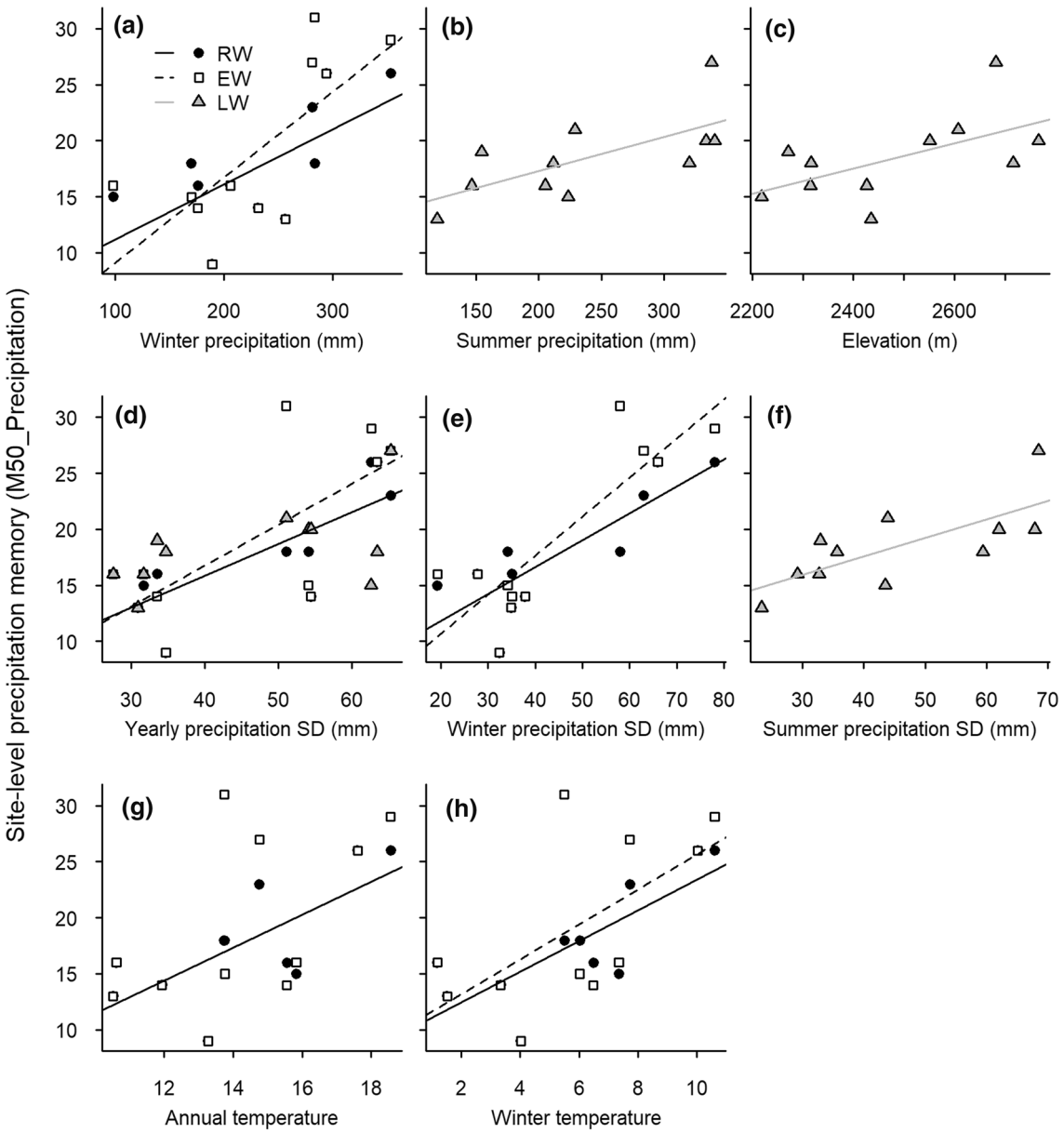

Fig. 3 Linear regressions between site-level precipitation memory (M_{50}; the month prior to December of the current year at which the cumulative weights first exceed 0.5) and **a** winter precipitation, **b** summer precipitation, **c** elevation, **d** yearly precipitation standard deviation (SD), **e** winter precipitation SD, **f** summer precipitation SD, **g** annual temperature, and **h** winter temperature. Only significant relationships are shown: symbols indicate $p < 0.01$, and regression lines indicate $p < 0.05$ (Table S4). Black circles/lines represent whole-ring widths (RW), *white squares/dashed lines* represent earlywood (EW), and *gray triangles/lines* represent latewood (LW)

However, the antecedent precipitation ($a_{s,3}$) effect for whole-ring widths was negatively correlated with annual (Fig. 4a), winter (Fig. 4b), and summer (Fig. 4c) precipitation totals ($R^2 = 0.60$, 0.69, and 0.27, respectively). The site-level earlywood and latewood precipitation ($a_{s,3}$) effects were also negatively correlated with annual, summer, and winter precipitation (earlywood $R^2 = 0.48$, 0.15, and 0.70, respectively; latewood $R^2 = 0.72$, 0.54, and 0.46, respectively).

Sites with higher annual and winter precipitation also had higher variability in annual and winter precipitation (Fig. S8), and the antecedent precipitation (P^{ant}) main effect ($a_{s,3}$) was strongly and negatively correlated with this variability (measured as standard deviation) in all three ring type models. That is, the higher the standard deviation in annual and winter precipitation, the less important antecedent precipitation was for growth (Table S3, Fig. 4d, e). The precipitation effect ($a_{s,3}$) for latewood growth was negatively

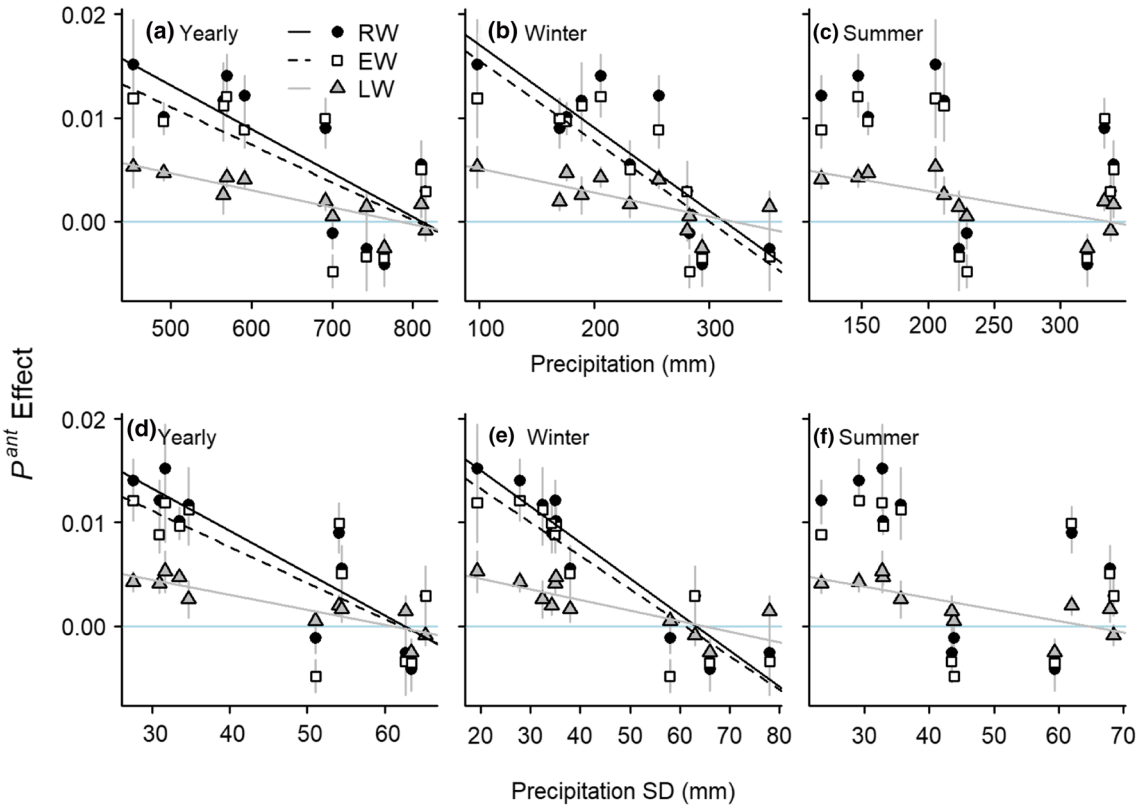

Fig. 4 Linear regressions between site-level antecedent precipitation (P^{ant}) main effects ($a_{s,3}$) and **a** annual, **b** winter, **c** summer precipitation, **d** annual, **e** winter, and **f** summer precipitation standard deviation. All relationships with regression lines are significant ($p < 0.05$; Table S3). *Black circles/lines* represent whole-ring widths, *white squares/dashed lines* represent earlywood, and *gray triangles/lines* represent latewood. *Blue lines* cross the *y*-axis at 0. Whiskers depict 95% Bayesian credible intervals

correlated with the standard deviation of summer precipitation (Table S3, Fig. 4f). The antecedent temperature (T^{ant}) main effect ($a_{s,4}$) and the $P^{ant} \times T^{ant}$ interaction effect ($a_{s,5}$) generally did not correlate with indices of annual and seasonal precipitation amount or variation (Table S3), except for that the temperature effect ($a_{s,4}$) for whole ring and earlywood growth was negatively correlated with summer temperature ($p < 0.1$, Table S3).

Discussion

Over what time scales are climate influences on tree growth evident?

The trees in this study were sampled "ecologically" rather than for climate reconstruction, which means they were not in particularly harsh conditions or near the edge of their range (Nehrbass-Ahles et al. 2014), although they still occurred in semi-arid sites in the southwestern US. Across all sites, the climate memory of tree growth was relatively long; while climate conditions in the year of ring formation and 1 year prior were generally most important for annual and sub-annual growth, climate conditions two, three, and four years prior to ring formation were also influential. These results are consistent with other studies in the Southwest that used International Tree-Ring Data Bank (ITRDB) records, from trees often collected for climate reconstruction purposes, to examine relationships between tree growth and climate at comparable time scales (Peltier et al. 2018). Using conifer tree-ring records from the ITRDB in the Southwest, Peltier et al. (2018) employed the SAM approach and also found that precipitation and temperature importance weights were highest in the year of growth (accounting for nearly half the total weight) and the year prior to growth, but conditions 2–4 years prior to growth still continued to influence growth. It is significant that we found similar evidence for long climatic memory in trees using a different dataset collected for a different purpose, suggesting that long climatic memory in trees is a widespread phenomenon not limited to highly "sensitive" trees often chosen for paleo-climate reconstructions (Esper et al. 2015). We note evidence for long memory of past climate in tree growth has been found worldwide, with examples including *Pinus brutia* in the eastern Mediterranean, *P. pinea* in Italy, and multiple species in

the Spanish Pyrenees (Mazza and Manetti 2013; Marqués et al. 2021).

It is also worth pointing out that Szejner et al. (2020) found shorter legacies in carbon isotope ratios and ring-width index in these same sites, using Superposed Epoch Analysis (SEA) and detrended chronologies. There are several aspects that could explain these differences. First, our analytical model focused on individual core and tree-level patterns rather than within-site integration of individual chronologies, as used in Szejner et al. (2020). This difference likely rendered our analysis more sensitive to the responses of individual tree phenotypes (i.e., endogenous factors), whereas the Szejner et al. (2020) analysis was more sensitive to site-to-site and year-to-year climate variability (i.e., exogenous factors). Second, Szejner et al. (2020) found that current year conditions were most important for tree growth, which our analysis also generally shows (Fig. S4), but we also find that conditions during previous years are important. In our study, the high importance of prior year's climate also captured the influence of the winter months just preceding ring formation, which have been found to be important predictors of tree growth in other studies (e.g., Martin et al. 2018). Finally, we did not focus on the most extreme droughts as "key events" in this study, which is required in SEA. Rather, we analyzed the influence of climate on tree growth across the entire period of the record, including all drought events. It is possible that evidence of memory in drought sensitivity is most likely to be detected when assessed across many droughts of variable intensity, rather than when focused on the most extreme droughts. In analyses relying on the most extreme droughts, exogenous (climate-determined) lags might be so dominant as to obscure endogenous (phenotype-determined) lags. The latter might only emerge in analyses that include a broad range of climate system states assessed across many years.

The long climatic memory reported here and elsewhere likely reflects an indirect effect of past climate, mediated through various physical and physiological mechanisms. Possible mechanisms for such lagged effects of climate on tree growth include retention of canopy needles for several years, storage of non-structural carbohydrates (NSC) over multiple years, hydraulic damage from prior drought, and pest or pathogen associations with drought-stressed trees, among others (Peltier et al. 2018). *P. ponderosa* needles are usually retained for 3 to 4 years (Fritts 1976), meaning that an abundant or poor needle crop in a particular year could positively or negatively impact growth for several years. The role of NSC in lagged growth responses to climate is not fully understood. However, as average NSC pool ages can be nine or more years old in conifer species in temperate forests (Richardson et al. 2012), and old NSC (>15 years) can be accessible (Carbone 2013), such old NSC could represent a functional link between antecedent climate and current growth. Persistent hydraulic damage could also result in long-lasting effects from water stress, particularly if functional sapwood area is significantly reduced (Anderegg et al. 2015; Trugman et al. 2018; Peltier and Ogle 2019), or significant changes in functional canopy area occur (Jump et al. 2017). Finally, pests and pathogens are typically more successful in water-stressed trees (Jactel et al. 2012), providing another way that climate variability, coupled with insect outbreaks, can have long lasting consequences for tree vitality and growth (Peters et al. 2017). Physical effects may also be important; trees have access to deep soil water resources, which integrate precipitation inputs over multiple seasons, but which may also be depleted after severe drought events (Kerhoulas and Kane 2012; Rempe and Dietrich 2018). Lagged effects of climate on tree growth are increasingly recognized as important (e.g., Jiang et al. 2019), but focused experimental work is needed to understand the mechanisms by which tree rings integrate climate over multiple years.

Varying climate responses at different sites across a precipitation gradient illustrate the diversity of conditions experienced by *P. ponderosa* across the study region. A significant growth versus antecedent precipitation relationship, which we expected, was observed in eight of the 11 study sites (Fig. 2c). The lack of a direct effect of precipitation in two sites and a negative effect in one site could be due to a precipitation x temperature interaction, or unique precipitation distributions in the interannual sequence of the time series. These are both examples of possible exogenous influences on climate memory effects. The direct effect of temperature was more variable (Fig. 2d). Typically, temperature has a negative effect on tree growth in the Southwest because of its link to increased drought stress (Williams et al. 2013; Adams and Kolb 2005), which appears to occur in six sites. However, warmer temperatures were positively correlated with tree growth in two sites (sites 7 and 8), both of which are in the southern portion of the study area (Fig. 1) and are associated with comparatively high rainfall (Table S1) and high baseline growth (Fig. 2a). This suggests that when trees have access to greater soil moisture, higher antecedent temperatures lead to greater productivity, potentially due to the effect of warm, but not extreme, temperatures on physiological processes involved in carbon gain, allocation, and biomass production (Way and Oren 2010).

It is not surprising that antecedent temperature and precipitation interact to govern tree growth across the precipitation gradient in the Southwest. However, the net effect of this interaction indicates the existence of a synergistic impact leading to increased sensitivity of tree growth to the combination of hotter and drier conditions, or what might be referred to as hot drought (Overpeck 2013). This has been documented on a temporal scale where drier sites showed increasing growth sensitivity to PDSI over the last century,

paralleled by higher mortality following the ongoing drought in California (Keen et al. 2022). Similar changes in growth sensitivity to climate have been reported across precipitation gradients in different functional types (Kannenberg et al. 2021) and between different biomes (Hsu et al. 2012; Gherardi and Sala 2019; Maurer et al. 2020; O'Donnell et al. 2021). We would expect these trends to continue given projections of rising temperatures (Zobel et al. 2017).

Do tree growth sensitivity to climate and ecological memory vary across the precipitation gradient?

Relationships between tree growth and climate did vary across the precipitation gradient, but percent summer (monsoon) precipitation provided little insight into spatial variation in climate-growth relationships. We suggest that the NAM gradient is only one gradient among several in this complex region that governs tree and forest productivity (Gutzler 2004). We did find that the total amount of precipitation and associated monthly variation were important in influencing tree growth. Sites 5, 6, and 7 in central and southern Arizona (AZ) stood out in several analyses: they had the highest standard deviations in monthly precipitation (Table S1), they are 3 of the 4 wettest sites (Table S1), and they had 3 of the 4 lowest precipitation main effect sizes (Fig. 2c). The finding that these wet sites supported *P. ponderosa* trees with lower precipitation sensitivity, under average temperature conditions, is consistent with past studies and was expected. For example, Adams and Kolb (2005) found that tree growth of several conifer species in higher, wetter sites in AZ was less sensitive to drought than in lower, drier sites. The lower precipitation sensitivity of tree growth under average temperature conditions in these sites suggests that trees are following a conservative strategy, in which they are not exhibiting physiological plasticity that would permit increased or decreased growth to track shifting conditions. It is also possible that in these wetter sites something besides moisture (e.g., nutrient limitations or cloud cover) is limiting tree growth during wet periods such that additional precipitation does not result in high growth in very wet years (Chapin et al. 1987). Trees in drier sites are generally more sensitive to precipitation, indicating that they may be most affected by changes to the total amount or timing of precipitation (Anderegg et al. 2019).

In our study, lower climate sensitivity was associated with longer climatic memory (Fig. S7). This combination of low effect size and long memory implies a muted response to climate; trees in these variable sites are not responsive to every pulse of rain but integrate climate (e.g., precipitation pulses) over many seasons and years. In these sites, if a tree allocates additional carbon resources to roots, canopy expansion, or wider than average rings in a wet year, the wet year could have a long-lasting influence on tree growth. Alternately, when a dry year occurs, a poor needle crop (Fritts 1976) or a loss of roots (Brunner et al. 2015) may necessitate a longer recovery time; effects may be long-lasting even if subsequent years have abundant rainfall (e.g., Anderegg et al. 2015). Trees that receive less summer precipitation might have the ability to "immediately" take advantage of rain events, making their growth more sensitive to recent conditions (shorter memory, lower M_{50}). We might hypothesize that trees at these sites would have faster carbon cycling rates and younger NSC. The finding that higher climatic sensitivity is associated with shorter climatic memory is interesting in the context of the ongoing discussions about biases in the ITRDB (Klesse et al. 2018). First, any bias in ITRDB is likely in the magnitude of the climate-growth responses, and not in the direction or character of the relationships. In addition, short climatic memory of sensitive trees is a positive attribute for climate or disturbance reconstructions, since multi-year memory in tree rings can bias or contaminate climatic or disturbance signals (Esper et al. 2015, 2018).

Do earlywood and latewood growth differ in their sensitivities to climate and climatic memory?

For both climatic sensitivity and memory, site differences were readily apparent in earlywood growth attributes. However, latewood growth was fairly invariant across sites in terms of baseline growth under average conditions. This may be due to little variation in the onset of latewood formation in *P. ponderosa*, even in years with very different precipitation patterns (Ziaco et al. 2018). However, the finding of greater variability in earlywood widths may be species-specific; in some species, latewood widths vary more than earlywood widths, but in other species the opposite occurs (e.g., Miina 2000). Climatic memory was quite different between earlywood and latewood as well (Fig. S6); latewood memory was shorter and less variable between sites, but climate in years prior to growth was still important.

While climate influenced latewood growth, the strongest factor associated with low latewood growth was simply high earlywood growth (negative effect across all 11 sites). This should not be confused with positive correlations between raw earlywood and latewood widths, which are observed in simple bivariate plots or correlation analyses (Fig. S3, Meko and Baisan 2001; Griffin et al. 2011). Instead, this earlywood effect should be thought of as the conditional effect of earlywood growth given that climate, ring age, and past ring width effects are accounted for. This suggests that after accounting for the effects of climate, age, and past widths, which tend to have the same directional effects on earlywood and latewood growth, the conditional effect of earlywood on latewood growth is actually negative, pointing to a tradeoff between these two modes of radial growth. This tradeoff could be related to carbon resources; if a tree

invests a great deal of carbon in earlywood (or earlywood formation runs longer), there may be less carbon (or time) to invest in latewood growth. This idea is supported by isotopic analysis of the same trees used in this study; isotope signals in earlywood and latewood were generally positively correlated (Szejner et al. 2018), suggesting that trees use the same resources to produce earlywood and latewood. Alternatively, the tradeoff could be related to xylogenesis and phenology mechanisms (Ziaco et al. 2018). It is thought that earlywood is important for water transport and latewood is important for tree structure; each year's growth represents a balance between a tree's maintenance of these two functions of xylem (Björklund et al. 2017). Future research might explore whether allocation between these competing functions may be altered by recent climate conditions, particularly drought. For example, an adaptive strategy would be to invest relatively more carbon towards earlywood growth following severe cavitation events to efficiently regain pre-drought sapwood area (Trugman et al. 2018). Finally, the possibility of a carbon allocation tradeoff between earlywood and latewood has implications for climate reconstructions when using any type of tree-ring data: whole ring, earlywood, or latewood.

Conclusions

Our study of *Pinus ponderosa* in the Southwest showed that tree growth responses to climate and the time-scales over which growth responds to climate varied across the regional precipitation gradient. Severe summer drought has been observed over the period 2000–2018 (Williams et al. 2020) due to anthropogenic warming, and the North American Monsoon may experience changes such as a delayed onset and shifts in precipitation distribution to later in the season (Cook and Seager 2013). Our results suggest that such future changes to precipitation patterns will have unequal effects on tree growth across the regional precipitation gradient, with potential implications for tree growth and mortality, carbon storage, and regional species migrations.

Supplementary Information The online version contains supplementary material available at https://doi.org/10.1007/s00442-022-05156-1.

Acknowledgements We thank the Ogle lab group for feedback on earlier versions of this manuscript. This manuscript has been authored in part by UT-Battelle, LLC, under contract DE-AC05-00OR22725 with the US Department of Energy (DOE). The US government retains and the publisher, by accepting the article for publication, acknowledges that the US government retains a nonexclusive, paid-up, irrevocable, worldwide license to publish or reproduce the published form of this manuscript, or allow others to do so, for US government purposes. DOE will provide public access to these results of federally sponsored research in accordance with the DOE Public Access Plan (http://energy.gov/downloads/doe-public-access-plan).

Author contribution statement LLY and KO conceived of the idea. PS and RKM collected the data. LLY, KO and DP analyzed the data. LLY wrote the manuscript; all authors provided editorial advice.

Funding The majority of the work conducted in this study was funded by a National Science Foundation-Advances in Biological Informatics grant to K. Ogle (#1458867). P. Szejner and R. Monson acknowledge financial support from the Macrosystems Program in the Emerging Frontiers Section of the U.S. National Science Foundation (#1065790) and the Ecosystems Program in the Division of Environmental Biology (#1754430), which enabled much of the sampling and data collection. Y. Liu was partly supported by the U.S. Department of Energy contract DE-AC05-00OR22725.

Availability of data and material All data for this manuscript will be posted in the International Tree-Ring Database (ITRDB).

Code availability Code is available from corresponding author upon request.

Declarations

Conflict of interest The authors declare that they have no conflict of interest.

Ethics approval Ethics approval was not required for this study.

Consent to participate Not applicable.

Consent for publication Not applicable.

References

Adams DK, Comrie AC (1997) The North American monsoon. Bull Am Meteorol Soc 78:2197–2214. https://doi.org/10.1175/1520-0477(1997)078%3c2197:TNAM%3e2.0.CO;2

Adams HD, Kolb TE (2005) Tree growth response to drought and temperature in a mountain landscape in northern Arizona, USA. J Biogeogr 32:1629–1640. https://doi.org/10.1111/j.1365-2699.2005.01292.x

Adams DK, Minjarez C, Serra Y, Quintanar A, Alatore L, Granados A, Vásquez E, Braun J (2014) Mexican GPS tracks convection from North American Monsoon. Eos Trans Am Geophys Union 95:61–62. https://doi.org/10.1002/2014EO070001

Anderegg WRL, Schwalm C, Biondi F, Camarero JJ, Koch G, Litvak M, Ogle K, Shaw JD, Shevliakova E, Williams AP, Wolf A, Ziaco E, Pacala S (2015) Pervasive drought legacies in forest ecosystems and their implications for carbon cycle models. Science 349:528–532. https://doi.org/10.1126/science.aab1833

Anderegg WRL, Anderegg LDL, Kerr KL, Trugman AT (2019) Widespread drought-induced tree mortality at dry range edges indicates climate stress exceeds species' compensating mechanisms. Glob Change Biol 25:3793–3802. https://doi.org/10.1111/gcb.14771

Babst F, Wright WE, Szejner P, Wells L, Belmecheri S, Monson RK (2016) Blue intensity parameters derived from Ponderosa pine tree rings characterize intra-annual density fluctuations and reveal seasonally divergent water limitations. Trees 30:1403–1415. https://doi.org/10.1007/s00468-016-1377-6

Belmecheri S, Wright WE, Szejner P, Morino KA, Monson RK (2018) Carbon and oxygen isotope fractionations in tree rings reveal interactions between cambial phenology and seasonal climate.

Plant Cell Environ 41:2758–2772. https://doi.org/10.1111/pce.13401
Björklund J, Seftigen K, Schweingruber F, Fonti P, von Arx G, Bryukhanova MV, Cuny HE, Carrer M, Castagneri D, Frank DC (2017) Cell size and wall dimensions drive distinct variability of earlywood and latewood density in Northern Hemisphere conifers. New Phytol 216:728–740. https://doi.org/10.1111/nph.14639
Brunner I, Herzog C, Dawes MA, Arend M, Sperisen C (2015) How tree roots respond to drought. Front Plant Sci 6:547. https://doi.org/10.3389/fpls.2015.00547
Chapin FS, Bloom AJ, Field CB, Waring RH (1987) Plant responses to multiple environmental factors. BioScience 37:49–57
Cook BI, Seager R (2013) The response of the North American Monsoon to increased greenhouse gas forcing. JGR Atmospheres 118:1690–1699. https://doi.org/10.1002/jgrd.50111
Douglas MW, Maddox RA, Howard K, Reyes S (1993) The Mexican Monsoon. J Clim 6:1665–1677. https://doi.org/10.1175/1520-0442(1993)006%3c1665:TMM%3e2.0.CO;2
Esper JL, Schneider L, Smerdon JE, Schöne BR, Büntgen U (2015) Signals and memory in tree-ring width and density data. Dendrochronologia 35:62–70. https://doi.org/10.1016/j.dendro.2015.07.001
Esper J, St. George S, Anchukaitis K, D'Arrigo R, Ljungqvist FC, Luterbacher J, Schneider L, Stoffel M, Wilson R, Büntgen U (2018) Large-scale, millennial-length temperature reconstructions from tree-rings. Dendrochronologia 50:81–90. https://doi.org/10.1016/j.dendro.2018.06.001
Fritts HC (1976) Tree rings and climate. Academic Press, New York
Gherardi LA, Sala OE (2019) Effect of interannual precipitation variability on dryland productivity: a global synthesis. Glob Chang Biol 25:269–276. https://doi.org/10.1111/gcb.14480
Griffin D, Meko DM, Touchan R, Leavitt SW, Woodhouse CA (2011) Latewood chronology development for summer-moisture reconstruction in the US Southwest. Tree-Ring Res 67:87–101. https://doi.org/10.3959/2011-4.1
Griffin D, Woodhouse CA, Meko DM, Stahle DW, Faulstich HL, Carrillo C, Touchan R, Castro CL, Leavitt SW (2013) North American monsoon precipitation reconstructed from tree-ring latewood. Geophys Res Lett 40:954–958. https://doi.org/10.1002/grl.50184
Guo JS, Hultine KR, Koch GW, Kropp H, Ogle K (2020) Temporal shifts in iso/anisohydry revealed from daily observations of plant water potential in a dominant desert shrub. New Phytol 225:713–726. https://doi.org/10.1111/nph.16196
Gutzler DS (2004) An index of interannual precipitation variability in the core of the North American Monsoon region. J Climate 17:4473–4480. https://doi.org/10.1175/3226.1
Higgins RW, Yao Y, Wang XL (1997) Influence of the North American Monsoon System on the U.S. summer precipitation regime. J Climate 10:2600–2622. https://doi.org/10.1175/1520-0442(1997)010%3c2600:IOTNAM%3e2.0.CO;2
Higgins RW, Chen Y, Douglas AV (1999) Interannual variability of the North American warm season precipitation regime. J Clim 12:653–680. https://doi.org/10.1175/1520-0442(1999)012%3c0653:IVOTNA%3e2.0.CO;2
Higgins RW, Douglas A, Hahmann A, Berbery EH, Gutzler D, Shuttleworth J, Stensrud D, Amador J, Carbone R, Cortez M, Douglas M, Lobato R, Meitin J, Ropelewski C, Schemm J, Schubert S, Zhang C (2003) Progress in Pan American CLIVAR Research: The North American Monsoon System. Atmósfera 16:29–65
Hsu JS, Powell J, Adler PB (2012) Sensitivity of mean annual primary production to precipitation. Glob Change Biol 18:2246–2255. https://doi.org/10.1111/j.1365-2486.2012.02687.x
Jactel H, Petit J, Desprez-Loustau ML, Delzon S, Piou D, Battisti A, Koricheva J (2012) Drought effects on damage by forest insects and pathogens: a meta-analysis. Glob Change Biol 18:267–276. https://doi.org/10.1111/j.1365-2486.2011.02512.x
Jiang P, Liu H, Piao S, Ciais P, Wu X, Yin Y, Wang H (2019) Enhanced growth after extreme wetness compensates for post-drought carbon loss in dry forests. Nat Commun 10:195. https://doi.org/10.1038/s41467-018-08229-z
Jump AS, Ruiz-Benito P, Greenwood S, Allen CD, Kitzberger T, Fensham R, Martínez-Vilalta J, Lloret F (2017) Structural overshoot of tree growth with climate variability and the global spectrum of drought-induced forest dieback. Glob Change Biol 23:3742–3757. https://doi.org/10.1111/gcb.13636
Kannenberg SA, Driscoll A, Szejner P, Anderegg W, Ehleringer J (2021) Rapid increases in shrubland and forest intrinsic water-use efficiency during an ongoing megadrought. Proc Natl Acad Sci USA 118(52):e2118052118. https://doi.org/10.1073/pnas.2118052118
Keen RM, Voelker SL, Wang SYS, Bentz BJ, Goulden M, Dangerfield CR, Reed CC, Hood SM, Csank AZ, Dawson TE, Merschel AG, Still CJ (2022) Changes in tree drought sensitivity provided early warning signals to the California drought and forest mortality event. Glob Change Biol 28:1119–1132. https://doi.org/10.1111/gcb.15973
Kerhoulas LP, Kane JM (2012) Sensitivity of ring growth and carbon allocation to climatic variation vary within ponderosa pine trees. Tree Physiol 32:14–23. https://doi.org/10.1093/treephys/tpr112
Klesse S, DeRose RJ, Guiterman CH, Lynch AM, O'Connor CD, Shaw JD, Evans MEK (2018) Sampling bias overestimates climate change impacts on forest growth in the SW United States. Nat Commun 9:5336
Liu Y, Schwalm CR, Samuels-Crow KE, Ogle K (2019) Ecological memory of daily carbon exchange across the globe and its importance in drylands. Ecol Lett 22:1806–1816. https://doi.org/10.1111/ele.13363
Marqués L, Peltier DMP, Camarero J, Zavala MA, Madrigal-González J, Sangüesa-Barreda G, Ogle K (2021) Disentangling the legacies of climate and management on tree growth. Ecosystems. https://doi.org/10.1007/s10021-021-00650-8
Martin J, Looker N, Hoylman Z, Jencso K, Hu J (2018) Differential use of winter precipitation by upper and lower elevation Douglas fir in the Northern Rockies. Glob Change Biol 24:5607–5621. https://doi.org/10.1111/gcb.14435
Maurer GE, Hallmark AJ, Brown RF, Sala OE, Collins SL (2020) Sensitivity of primary production to precipitation across the United States. Ecol Lett 23:527–536. https://doi.org/10.1111/ele.13455
Mazza G, Manetti MC (2013) Growth rate and climate responses of *Pinus pinea* L. in Italian coastal stands over the last century. Clim Change 121:713–725. https://doi.org/10.1007/s10584-013-0933-y
McDowell NG, Allen CD, Marshall L (2010) Growth, carbon-isotope discrimination, and drought-associated mortality across a *Pinus ponderosa* elevational transect. Glob Change Biol 16:399–415. https://doi.org/10.1111/j.1365-2486.2009.01994.x
Meko DM, Baisan CH (2001) Pilot study of latewood-width of conifers as an indicator of variability of summer rainfall in the North American monsoon region. Int J Climatol 21:697–708. https://doi.org/10.1002/joc.646
Miina J (2000) Dependence of tree-ring, earlywood and latewood indices of Scots pine and Norway spruce on climatic factors in eastern Finland. Ecol Model 132:259–273. https://doi.org/10.1016/S0304-3800(00)00296-9
Monson RK, Szejner P, Belmecheri S, Morino K, Wright WE (2018) Finding the seasons in tree ring stable isotopes. Am J Bot 105:819–821. https://doi.org/10.1002/ajb2.1083
Nehrbass-Ahles C, Babst F, Klesse S, Nötzli M, Bouriaud O, Neukom R, Dobbertin M, Frank D (2014) The influence of sampling design

on tree-ring-based quantification of forest growth. Glob Change Biol 20:2867–2885. https://doi.org/10.1111/gcb.12599
Neilson RP (1987) Biotic regionalization and climatic controls in western North America. Vegetatio 70:135–147. https://doi.org/10.1007/BF00039327
O'Donnell AJ, Renton M, Allen KJ, Grierson PF (2021) Tree growth responses to temporal variation in rainfall differ across a continental-scale climatic gradient. PLoS One 16:e0249959. https://doi.org/10.1371/journal.pone.0249959
Ogle K, Barber JJ, Barron-Gafford GA, Bentley LP, Young JM, Huxman TE, Loik ME, Tissue DT (2015) Quantifying ecological memory in plant and ecosystem processes. Ecol Lett 18:221–235. https://doi.org/10.1111/ele.12399
Overpeck JT (2013) Climate science: the challenge of hot drought. Nature 503:350–351. https://doi.org/10.1038/503350a
Peltier DMP, Ogle K (2019) Legacies of La Niña: North American monsoon can rescue trees from winter drought. Glob Change Biol 25:121–133. https://doi.org/10.1111/gcb.14487
Peltier DMP, Fell M, Ogle K (2016) Legacy effects of drought in the southwestern United States: a multi-species synthesis. Ecol Monogr 86:312–326. https://doi.org/10.1002/ecm.1219
Peltier DMP, Barber JJ, Ogle K (2018) Quantifying antecedent climatic drivers of tree growth in the Southwestern US. J Ecol 106:613–624. https://doi.org/10.1111/1365-2745.12878
Peltier DMP, Guo J, Nguyen P, Bangs M, Gear L, Wilson M, Jefferys S, Samuels-Crow K, Yocom LL, Liu Y, Fell MK, Auty D, Schwalm C, Anderegg WRL, Koch GW, Litvak ME, Ogle K (2022) Temperature memory and non-structural carbohydrates mediate legacies of a hot drought in trees across the southwestern USA. Tree Physiol 42:71–85. https://doi.org/10.1093/treephys/tpab091
Peters RL, Klesse S, Fonti P, Frank DC (2017) Contribution of climate vs. larch budmoth outbreaks in regulating biomass accumulation in high-elevation forests. For Ecol Manag 401:147–158. https://doi.org/10.1016/j.foreco.2017.06.032
Plummer M, Best N, Cowles K, Vines K (2006) CODA: convergence diagnosis and output analysis for MCMC. R News 6:7–11
Plummer M (2003) JAGS: A program for analysis of Bayesian graphical models using Gibbs sampling. 3rd international workshop on distributed statistical computing. Vienna
Plummer M (2013) rjags-package: Bayesian graphical models using MCMC in rjags: Bayesian Graphical Models using MCMC
PRISM Climate Group (2018) Climate data. http://prism.oregonstate.edu/
R Core Team (2021) R: A Language and Environment for Statistical Computing. R Foundation for Statistical Computing
Rempe DM, Dietrich WE (2018) Direct observations of rock moisture, a hidden component of the hydrologic cycle. Proc Natl Acad Sci USA 115:2664–2669. https://doi.org/10.1073/pnas.1800141115
Richardson AD, Carbone MS, Keenan TF, Czimczik CI, Hollinger DY, Murakami P, Schaberg PG, Xu X (2012) Seasonal dynamics and age of stemwood NSCs in temperate forests. New Phytol 197:850–861
Salzer MW, Kipfmueller KF (2005) Reconstructed temperature and precipitation on a millennial timescale from tree-rings in the southern Colorado Plateau, U.S.A. Clim Change 70:465–487. https://doi.org/10.1007/s10584-005-5922-3
Stahle DW, Cleaveland MK, Grissino-Mayer HD, Griffin RD, Fye FK, Therrell MD, Burnette DJ, Meko DM, Villanueva Diaz J (2009) Cool- and warm-season precipitation reconstructions over western New Mexico. J Clim 22:3729–3750. https://doi.org/10.1175/2008JCLI2752.1
Stokes MA, Smiley TL (1968) An introduction to tree-ring dating. University of Chicago Press, Chicago
Szejner P, Wright WE, Babst F, Belmecheri S, Trouet V, Leavitt SW, Ehleringer JR, Monson RK (2016) Latitudinal gradients in tree ring stable carbon and oxygen isotopes reveal differential climate influences of the North American Monsoon System. J Geophy Res Biogeosci 121:1978–1991. https://doi.org/10.1002/2016JG003460
Szejner P, Wright WE, Belmecheri S, Meko D, Leavitt SW, Ehleringer JR, Monson RK (2018) Disentangling seasonal and interannual legacies from inferred patterns of forest water and carbon cycling using tree-ring stable isotopes. Glob Change Biol 24:5332–5347. https://doi.org/10.1111/gcb.14395
Szejner P, Belmecheri S, Ehleringer JR, Monson RK (2020) Recent increases in drought frequency cause observed multi-year drought legacies in the tree rings of semi-arid forests. Oecologia 192:241–259. https://doi.org/10.1007/s00442-019-04550-6
Trugman AT, Detto M, Bartlett MK, Medvigy D, Anderegg WRL, Schwalm C, Schaffer B, Pacala SW (2018) Tree carbon allocation explains forest drought-kill and recovery patterns. Ecol Lett 21:1552–1560. https://doi.org/10.1111/ele.13136
Way DA, Oren R (2010) Differential responses to changes in growth temperature in trees from different functional groups and biomes: a review and synthesis of data. Tree Physiol 30:669–688. https://doi.org/10.1093/treephys/tpq015
Williams AP, Allen CD, Macalady AK, Griffin D, Woodhouse CA, Meko DM, Swetnam TW, Rauscher SA, Seager R, Grissino-Mayer HD, Dean JS, Cook ER, Gangodagamage C, Cai M, McDowell NG (2013) Temperature as a potent driver of regional forest drought stress and tree mortality. Nat Clim Change 3:292–297. https://doi.org/10.1038/nclimate1693
Williams AP, Cook ER, Smerdon JE, Cook BI, Abatzoglou JT, Bolles K, Baek SH, Badger AM, Livneh B (2020) Large contribution from anthropogenic warming to an emerging North American megadrought. Science 368:314–318. https://doi.org/10.1126/science.aaz9600
Zhang W, Shi J, Zhao Y, Shi S, Ma X, Zhu Y (2021) December-March temperature reconstruction from tree-ring earlywood width in southeastern China during the period of 1871–2016. Int J Biometeorol 65:883–894. https://doi.org/10.1007/s00484-020-02067-9
Ziaco E, Truettner C, Biondi F, Bullock S (2018) Moisture-driven xylogenesis in *Pinus ponderosa* from a Mojave Desert mountain reveals high phenological plasticity. Plant Cell Environ 41:823–836. https://doi.org/10.1111/pce.13152
Zobel Z, Wang J, Wuebbles J, Rao Kotamarthi V (2017) High-resolution dynamical downscaling ensemble projections of future extreme temperature distributions for the United States. Earth's Future 5:1234–1251. https://doi.org/10.1002/2017EF000642